$S_1\ ^1A_2(n\pi^*)$ and $S_2\ ^1A_1(\pi\pi^*)$ States of Jet-Cooled Xanthone

Yukio Ohshima, Teruyuki Fujii, Takanori Fujita, and Daisuke Inaba

Graduate School of Human and Environmental Studies, Kyoto University, Kyoto 606-8501, Japan

Masaaki Baba*

Department of Chemistry, Graduate School of Science, Kyoto University, Kyoto 606-8501, Japan

Received: February 27, 2003; In Final Form: July 14, 2003

The $S_1\ ^1A_2(n\pi^*)$ and $S_2\ ^1A_1(\pi\pi^*)$ states of xanthone are phosphorescent due to strong coupling with the triplet state. To investigate the mechanism of intersystem crossing, we observed the phosphorescence excitation spectrum of xanthone in a supersonic jet. The $S_1\ ^1A_2(n\pi^*) \leftarrow S_0$ transition shows a well-resolved structure with sharp vibronic bands. Prominent bands are assigned to out-of-plane vibrational bands, of which the intensities arise from the vibronic interaction with the $S_2\ ^1A_1(\pi\pi^*)$ state. The vibronic bands of the $S_2\ ^1A_1(\pi\pi^*) \leftarrow S_0$ transition are significantly broadened (55 cm^{-1}) and the band shape is Lorentzian. It indicates that the intersystem crossing is very fast from the $S_2\ ^1A_1(\pi\pi^*)$ state. The rate of intersystem crossing from the $S_2\ ^1A_1(\pi\pi^*)$ state is estimated to be 1.0×10^{13} s^{-1}.

I. Introduction

Electronically excited molecules are of great interest because of their roles in various dynamical processes. In particular, triplet states play important roles in many systems.[1] Low excited states of aromatic hydrocarbons such as polyacenes are the $\pi\pi^*$ states. The triplet state is only weakly optically active because singlet−triplet interaction is expected to be weak, as shown by El-Sayed.[2] In contrast, aromatic carbonyl molecules are strongly phosphorescent and the triplet states of key molecules have been extensively studied in a supersonic jet[3−6] as well as in the solid phase.[7−10] This triplet activity is attributed to strong interaction between the $n\pi^*$and $\pi\pi^*$ states.[11,12] These two states are close in energy and consequently the singlet−triplet coupling becomes appreciably strong.

Xanthone (xanthen-9-one) is a typical example of aromatic carbonyl molecules in which the triplet states are quite important for excited-state dynamics.[13−29] It is necessary to investigate isolated molecules in order to fully understand the energy structure and the mechanism of dynamical processes. In this article we present the results of phosphorescence excitation spectrum of jet-cooled xanthone. We have already reported the spectrum of the $T_1\ ^3A_2(n\pi^*) \leftarrow S_0$ and $S_1\ ^1A_2(n\pi^*) \leftarrow S_0$ transitions which have sharp vibronic bands.[30] The transition energies are 25 808 and 26 939 cm^{-1}, respectively. We extended the measurements to the shorter wavelength region and found significant spectral broadening for the $S_2\ ^1A_1(\pi\pi^*)$ state. This is a typical feature of strong singlet−triplet coupling of a molecule at the statistical limit in terms of radiationless transitions. We report the experimental results and discuss the excited-state structure and the mechanism of intersystem crossing in isolated xanthone molecules.

II. Experimental Section

The experimental setup will be briefly given here because details have been described elsewhere.[6,30] Xanthone (Wako Chemical) was purified by recrystalization in ethanol and dried. The sample was reserved in a heated stainless steel container (150 °C). The vapor was mixed with Ar buffer gas (1.5 atm) and expanded in a high vacuum chamber through a pulsed nozzle. The duration of the jet pulse was 0.5 ms. The rotational temperature was estimated to be about 5 K. We used a dye laser (Lambda Physics, Scanmate, bandwidth 0.1 cm^{-1}) pumped by a pulsed Nd^{3+}:YAG laser (Spectra Physics, INDI 40, 120 mJ at 532 nm, 5 ns duration) as a light source. The output was frequency-doubled by a BBO crystal. We obtained ultraviolet light with a pulse energy of about 1 mJ. The bandwidth is about 0.2 cm^{-1}. This laser beam was crossed with the supersonic jet at right angles. Phosphorescence from the excited molecules was collected by using an elipsoidal reflecter and a lens to a gated photomultiplier tube (Hamamatsu R282), which is coaxial with the jet. This photomultiplier tube is sensitive from 300 to 650 nm and phosphorescence was detected without any color filter. The phosphorescence excitation spectrum was observed by scanning the wavelength of the laser light monitoring the phosphorescence intensity, which has been obtained by photon counting after the laser shot (100−200 μs) by using a photon counting system (Stanford Research SR 400).

III. Results and Discussion

We have observed the phosphorescence excitation spectrum of jet-cooled xanthone in the wavelength region from 305 to 375 nm. The results are shown in Figure 1. The band at 371.10 nm (26939 cm^{-1}) is assigned to the 0_0^0 band of the $S_1\ ^1A_2(n\pi^*) \leftarrow S_0$ transition. The spectrum is composed of several sharp vibrational bands and becomes congested as the vibrational energy increases. Far more intense bands are observed in the 325−305 nm region. These bands are assigned to the $S_2\ ^1A_1(\pi\pi^*) \leftarrow S_0$ transition. The strong 325.45 nm (30 718 cm^{-1}) band is assigned as the 0_0^0 band. In our previous report, we tentatively assigned the 29 383 cm^{-1} band as this origin band.[30] However, this proved by the extensive measurement to be one of the vibronic bands of the $S_1\ ^1A_2(n\pi^*) \leftarrow S_0$ transition. The

* To whom correspondence should be addressed. E-mail: baba@ihsc.mbox.media.kyoto-u.ac.jp.

10.1021/jp030260d CCC: $25.00
Published on Web 09/27/2003

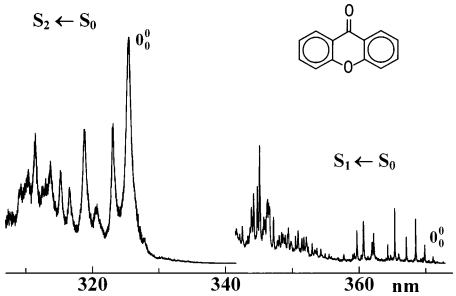

Figure 1. Phosphorescence excitation spectrum of xanthone in a supersonic jet.

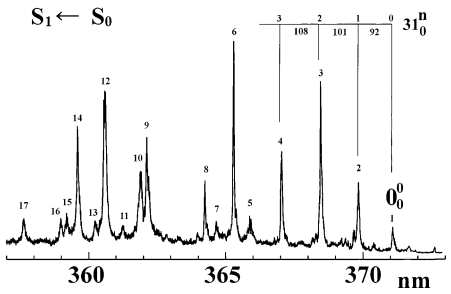

Figure 2. Expended spectrum in the lower energy region of the S_1 $^1A_2(n\pi^*) \leftarrow S_0$ transition.

TABLE 1: Observed Bands of the S_1 $^1A_2(n\pi^*) \leftarrow S_0$ Transition and Assignments

	transition wavenumber, cm^{-1}	vibrational frequency, cm^{-1}	assignment
1	26 939	0	0_0^0
2	27 031	92	31_0^1 (a_2)
3	27 132	193	31_0^2 (a_2)
4	27 240	301	31_0^3 (a_2)
5	27 321	382	
6	27 364	425	29_0^1 (a_2)
7	27 409	470	
8	27 441	502	28_0^1 (a_2)
9	27 608	669	36_0^1 (b_1)?
10	27 627	688	27_0^1 (a_2)
11	27 675	736	
12	27 725	786	26_0^1 (a_2)
13	27 755	816	
14	27 804	865	25_0^1 or 29_0^2 (a_2)
15	27 833	894	
16	27 849	910	
17	27 955	1016	

29 383 cm^{-1} band is not very strong in this measurement where the longer lifetime component is detected.

We observed both the $^1n\pi^*$ and $^1\pi\pi^*$ transitions whose spectral features are obviously different. We observed sharp vibronic bands for the S_1 $^1A_2(n\pi^*) \leftarrow S_0$ transition. The expanded spectrum in the lower energy region is shown in Figure 2 and the observed transition wavenumbers are summarized in Table 1. To assign the vibrational bands, we calculated the harmonic vibrational frequencies (in wavenumbers) of the S_1 $^1A_2(n\pi^*)$ state using the GAUSSIAN 98 program.[31] We performed the molecular-orbital calculations by spin restricted configuration interactions for a single excitation using a 6-31G(d,p) basis set (RCIS/6-31G(d,p)). We used the scaling factor value of 0.8970 recommended by Scott and Radom.[32] The results are summarized in Table 2. The calculation for the ground state has been reported by Connors and Fratini.[33]

TABLE 2: Calculated Vibrational Frequencies (in Wavenumbers) of Xanthone

symmetry	number	vibrational type[a]	S_0 $^1A_1$[b]	S_1 $^1A_2$[c]	S_2 $^1A_1$[c]
a_1	1	C-H stretch	3102	3038	3054
	2		3099	3033	3045
	3		3085	3021	3033
	4		3072	3009	3020
	5	C═O stretch	1682	1615	1619
	6	skeletal deform	1609	1594	1588
	7		1581	1506	1509
	8	C−H bend + skeletal deform	1471	1467	1459
	9		1450	1440	1427
	10		1326	1271	1316
	11		1259	1197	1258
	12		1201	1192	1207
	13		1160	1125	1143
	14		1134	1092	1130
	15		1095	1078	1073
	16		1015	1011	988
	17		817	803	819
	18	ring deform	685	676	653
	19		640	634	628
	20	C═O bend	508	479	484
	21	skeletal deform	371	359	370
	22		223	221	218
a_2	23	oop C−H wag	959	992	961
	24		936	953	901
	25		848	862	858
	26		752	758	718
	27		702	701	606
	28	oop ring bend	510	530	477
	29		447	440	397
	30	oop skeletal bend	238	250	221
	31	oop ring torsion	117	117	108
b_1	32	oop C−H wag	959	992	950
	33		937	954	888
	34		853	865	822
	35		785	756	720
	36		743	698	630
	37		656	542	535
	38	oop ring bend	529	449	482
	39		405	298	318
	40		281	227	248
	41	oop C═O wag	146	97	144
	42	oop ring wag	63	28	64
b_2	43	C−H stretch	3101	3038	3052
	44		3098	3032	3041
	45		3085	3021	3033
	46		3072	3008	3019
	47	skeletal deform	1597	1587	1562
	48		1558	1568	1511
	49		1457	1467	1476
	50	C−H bend + skeletal deform	1449	1428	1416
	51		1333	1279	1366
	52		1305	1257	1345
	53		1224	1195	1288
	54		1201	1171	1198
	55		1139	1084	1119
	56		1086	1070	1055
	57		1019	1019	1006
	58		911	876	901
	59		864	840	894
	60	ring deform	618	602	597
	61		578	557	572
	62		430	420	457
	63	C═O bend	309	279	300

[a] oop = out-of-plane. [b] The results of B3-LYP/6-31G(d,p) level are scaled by 0.9614. [c] The results of RCIS/6-31G(d,p) level are scaled by 0.8970.

For comparison we performed the density functional theory (DFT) calculation using the Becke three-parameter exchange functional (B3)[34] and the gradient correlated functional of Lee,

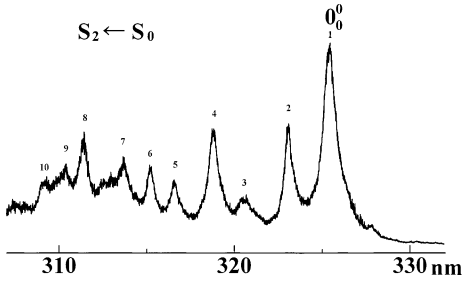

Figure 3. Expanded spectrum of the S_2 $^1A_1(\pi\pi^*) \leftarrow S_0$ transition.

Yang, and Parr (LYP)[35] with a 6-31G(d,p) basis set (B3LYP/6-31G(d,p)). We used the scaling factor of 0.9614.[32] The results are also shown in Table 2. Using these calculated vibrational frequencies we assigned the observed vibrational bands shown in Table 1. The S_1 $^1A_2(n\pi^*) \leftarrow S_0$ transition is symmetry forbidden in C_{2v}. The observed bands are considered to gain their intesities from the S_2 $^1A_1(\pi\pi^*) \leftarrow S_0$ transition by vibronic interaction between these two singlet excited states. The energy gap is 3779 cm^{-1}. Consequently, the out-of-plane a_2 mode vibrations are expected to be dominant in the spectrum. The 0_0^0 band is accompanied by 92, 193, and 301 cm^{-1} bands. These are assigned as the progression bands of $\nu_{31}(a_2)$ ring torsion vibration. However, the energy splitting slightly increases with the vibrational quantum number. This is positive anharmonicity which has been found in the case of strong vibronic coupling between the excited states.[36,37] The vibrational levels in the S_1 $^1A_2(n\pi^*)$ state of xanthone are considered to be shifted by the vibronic interaction with the S_2 $^1A_1(\pi\pi^*)$ state. Other prominent bands are also assigned to be the a_2 vibronic bands by using the results of calculations. We found a number of small peaks for the low-energy vibrational bands.[30] These satellite bands are considered as the triplet levels which gain the intensity by spin−orbit interaction with the singlet levels nearby.

These mixed levels emit phosphorescence, but no fluorescence could be observed in a supersonic jet. Therefore, the intersystem crossing is much faster than the fluorescence lifetime. The S_1 $^1A_2(n\pi^*)$ state does not directly couple with the T_1 $^3A_2(n\pi^*)$ state.[2] The energy of the T_2 $^3A_1(\pi\pi^*)$ state is known to be very close to that of the T_1 $^3A_2(n\pi^*)$ state in the solid phase.[13,15,16] The T_1 character drastically changes with host molecules and phosphorescence from both of the $^3A_2(n\pi^*)$ and $^3A_1(\pi\pi^*)$ states can be observed simultaneously.[14] These two triplet states are strongly coupled with the vibronic interaction. The energy gap between the T_1 $^3A_2(n\pi^*)$ and S_1 $^1A_2(n\pi^*)$ states is 1131 cm^{-1} for the isolated xanthone molecule.[30] The level densities of the mixed $^3n\pi^*$ and $^3\pi\pi^*$ states are sufficiently high at the energy of the S_1 $^1A_2(n\pi^*)$ state. Therefore, strong phosphorescence can be observed when we excite the vibronic levels in the S_1 $^1A_2(n\pi^*)$ state. The $^1n\pi^*$ state is strongly coupled with the mixed $^3n\pi^*$ and $^3\pi\pi^*$ levels and the molecule does not fluoresce, but phosphoresces strongly. It is considered to be difficult to observe phosphorescence from the $^3\pi\pi^*$ state in a supersonic jet because the lifetime is so long that the triplet molecule flies away from the detection region. The observed phosphorescence is, then, primarily from the $^3n\pi^*$ state.

The 0_0^0 band of the S_2 $^1A_1(\pi\pi^*) \leftarrow S_0$ transition is observed at 325.45 nm (30 718 cm^{-1}), which is followed by several vibronic bands. The expanded spectrum is shown in Figure 3. All the observed bands are remarkably broadened and the line shape is Lorentzian. We also calculated the vibrational frequencies in the S_2 $^1A_1(\pi\pi^*)$ state and the results are shown in Table 2. Using the results of the calculation, we assigned the vibronic bands of the S_2 $^1A_1(\pi\pi^*) \leftarrow S_0$ transition. The transition wavenumber, vibrational frequency, and assignment are summarized in Table 3. The S_2 $^1A_1(\pi\pi^*) \leftarrow S_0$ transition is an allowed strong transition of which the moment is along the C═O bond. The observed vibronic bands are of the totally symmetric a_1 vibrations. The S_2 $^1A_1(\pi\pi^*)$ state directly couples with the T_1 $^3A_2(n\pi^*)$ state, which is also mixed with the T_2 $^3A_1(\pi\pi^*)$ state. The density of coupling triplet levels is expected to be very high at the energy of the S_2 $^1A_1(\pi\pi^*)$ state where the excess energy of the T_1 $^3A_2(n\pi^*)$ state is 4910 cm^{-1}. Therefore, appreciably strong phosphorescence can be observed and the bandwidth is large due to the strong interaction with the triplet levels. Here we consider the energy dependence of the coupling triplet levels. The triplet level density is not very high in the lower energy region of the S_1 $^1A_2(n\pi^*)$ state. Weak satellite bands could be observed for the lower vibronic bands due to inhomogenity in the triplet manifold.[30] It is the intermediate case of a radiationless transition. This structure becomes continuous as the energy increases and the shape of each vibronic band becomes a broadened Lorentzian. The triplet level density is considered to be sufficiently high in the higher vibrational energy region (statistical limit).

TABLE 3: Observed Bands of the S_2 $^1A_1(\pi\pi^*) \leftarrow S_0$ Transition and Assignments

	transition wavenumber, cm^{-1}	vibrational frequency, cm^{-1}	assignment
1	30 718	0	0_0^0
2	30 941	223	22_0^1 (a_1)
3	31 174	456	20_0^1 (a_1)
4	31 354	636	18_0^1 (a_1)
5	31 579	861	$18_0^1 22_0^1$ (a_1)
6	31 719	1001	16_0^1 (a_1)
7	31 872	1154	13_0^1 (a_1)
8	32 099	1381	10_0^1 (a_1)
9	32 204	1486	
10	32 321	1603	

Bixon and Jortner[38] theoretically considered the band shape and the rate of intersystem crossing in the statistical limit. They assumed that the coupling triplet manifold is homogeneous, that is, the energy splitting (ϵ) and interaction strength (V) are constant for all the triplet levels. In this case the vibronic band has a Lorentzian shape

$$I(\nu - \nu_0) = \frac{1}{\pi} \frac{2/\Gamma}{(2/\Gamma)^2 + (\nu - \nu_0)^2} \tag{1}$$

and the bandwidth (fwhm) is given by

$$\Gamma = \pi\rho V^2 = \frac{\pi V^2}{\epsilon} \tag{2}$$

where $\rho = 1/\epsilon$ is the triplet level density. This bandwidth is also related with the rate of intersystem crossing (k) when we coherently excite all the coupled levels

$$\Gamma = \frac{k}{2\pi c} \tag{3}$$

The observed bandwidth of the S_2 $^1A_1(\pi\pi^*) \leftarrow S_0$ 0_0^0 band is 55 cm^{-1}. It indicates that the rate of intersystem crossing is 1.0×10^{13} s^{-1} and the lifetime ($\tau = 1/k$) is 96 fs. For instance, if we assume $\rho = 10^4$ cm, the interaction strength V is estimated to be 0.04 cm^{-1}. The bandwidth is proportional to the triplet

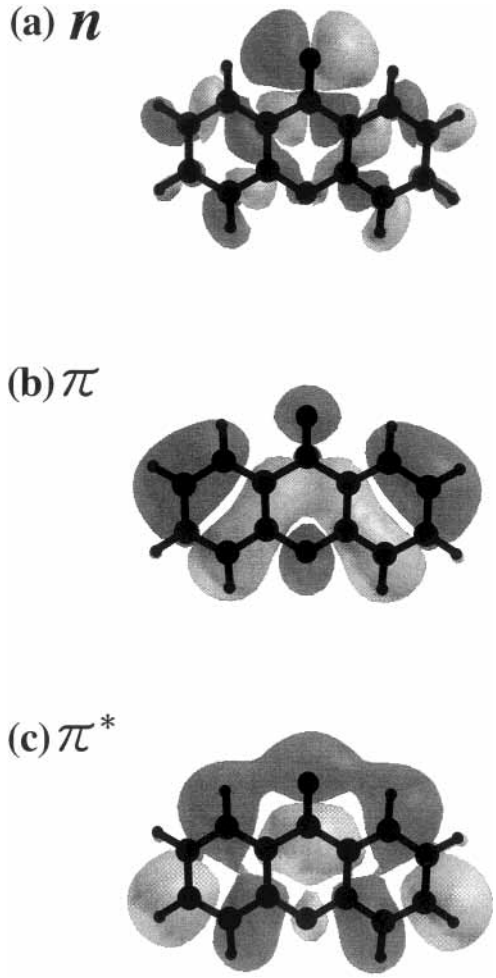

Figure 4. (a) n, (b) π, and (c) π^* orbitals obtained by calculation at the RCIS/6-31G(d,p) level.

level density ρ. It rapidly increases with the excess energy. The level density is expected to be fairly high at the energy of the $S_2\ ^1A_1(\pi\pi^*)$ state. Therefore, the bandwidth of the $S_2\ ^1A_1(\pi\pi^*) \leftarrow S_0$ transition is much larger than that for $S_1\ ^1A_2(n\pi^*) \leftarrow S_0$ transition. However, the observed bandwidth is almost constant for all the vibronic bands. It suggests that the assumption of homogeneous triplet levels is not fully valid for the present S_2-T_1 interaction.

Finally we discuss the electronic structure of aromatic carbonyl molecules such as xanthone and benzaldehyde. The most important thing is proximity of the $n\pi^*$ and $\pi\pi^*$ states. If we assume a pure $n \rightarrow \pi^*$ electronic excitation, the energy of the $n\pi^*$ state must be much lower than the $\pi\pi^*$ state, because the n orbital is the 2p orbital of an oxygen atom and the bonding energy is much smaller than the π orbital. However, the $n\pi^*$ and $\pi\pi^*$ states are very close in energy in aromatic carbonyl molecules. It is necessary to consider the characteristics of the eigenfunctions. The n,π and π^* orbitals obtained by calculation at the RCIS/6-31G(d,p) level of theory are illustrated in Figure 4. It is clearly seen that the n orbital is combined with σ orbitals and is delocalized over the whole molecule. The σ orbital has large bonding energy and this "$n-\sigma$" or in-plane orbital is lowered to nearly the same energy as the π orbital. The energy of the π orbital is raised by conjugation which reduces the bonding energy. Consequently, the $n\pi^*$ and $\pi\pi^*$ states of aromatic carbonyl molecules are close in energy. The delocalization of n orbital is expected to be more effective in large molecules such as xanthone and the spin−orbit interaction becomes stronger.

IV. Summary

Phosphorescence excitation spectrum of jet-cooled xanthone has been observed. The $S_1\ ^1A_2(n\pi^*) \leftarrow S_0$ transition is composed of weak 0_0^0 and sharp vibronic bands. This transition is forbidden and the intensity arises from vibronic interaction with the $S_2\ ^1A_1(\pi\pi^*)$ state. The prominent bands are of a_2 out-of-plane vibration which couples the $S_1\ ^1A_2(n\pi^*)$ and $S_2\ ^1A_1(\pi\pi^*)$ states. The vibronic bands of the $S_2\ ^1A_1(\pi\pi^*) \leftarrow S_0$ transition are remarkably broadened due to strong interaction with the triplet levels. The observed bandwidth is 55 cm^{-1} and the rate of intersystem crossing is $1.0 \times 10^{13}\ s^{-1}$. The $S_2\ ^1A_1(\pi\pi^*)$ state is directly coupled with the $T_1\ ^3A_2(n\pi^*)$ state and strong phosphorescence could be observed in a supersonic jet.

Aromatic carbonyl molecules are strongly phosphorescent, and the triplet activity is attributed to interaction between the closely located $n\pi^*$ and $\pi\pi^*$ states. The $T_2\ ^3A_1(\pi\pi^*)$ state is expected to be close in energy with the $T_1\ ^3A_2(n\pi^*)$ state. This is the main cause of fast intersystem crossing in xanthone and other aromatic carbonyl molecules as well. The n orbital is the atomic p orbital and the energy of the $n\pi^*$ state is expected to be much lower than that of the $\pi\pi^*$ state. However, the energy of the n orbital is lowered by mixing with the σ orbital. On the contrary, the energy of the π orbital is raised because the π bonding energy is reduced by conjugation in the aromatic carbonyl molecule. These result in proximity of the $n\pi^*$ and $\pi\pi^*$ states. To confirm it, extensive studies of phosphorescence excitation spectroscopy of other substituted molecules are desired.

Acknowledgment. This work is supported by a Grant-in-Aid for Scientific Research from the Ministry of Education, Culture, Sports, Science, and Technology of Japan.

References and Notes

(1) Avouris, P.; Gelbart, W. M.; El-Sayed, M. A. *Chem. Rev.* **1977**, *77*, 793.
(2) El-Sayed, M. A. *J. Chem. Phys.* **1963**, *38*, 2834.
(3) Holtzclaw, K. W.; Pratt, D. W. *J. Chem. Phys.* **1986**, *84*, 4713.
(4) Ohmori, N.; Suzuki, T.; Ito, M. *J. Phys. Chem.* **1988**, *92*, 1086.
(5) Sneh, O.; Cheshnovsky, O. *J. Phys. Chem.* **1991**, *95*, 7154.
(6) Kiritani, M.; Yoshii, T.; Hirota, N.; Baba, M. *J. Phys. Chem.* **1994**, *98*, 11 265.
(7) Niizuma, S.; Hirota, N. *J. Phys. Chem.* **1978**, *82*, 453.
(8) Harrigan, E. T.; Hirota, N. *Mol. Phys.* **1976**, *31*, 681.
(9) Baba, M. *J. Chem. Phys.* **1985**, *83*, 3318.
(10) Koyanagi, M.; Futami, H.; Nakashima, K. *J. Chem. Phys.* **1988**, *89*, 2662.
(11) McGlynn, S. P.; Azumi, T.; Kinoshita, M. *Molecular Spectroscopy of the Triplet State;* Prentice Hall: Englewood Cliffs, NJ, 1969.
(12) Goodman, L. *Excited State;* Lim, E. C., Ed.; Academic Press: New York, 1974; Vol. 1.
(13) Chakrabarti, A.; Hirota, N. *J. Phys. Chem.* **1976**, *80*, 2966.
(14) Vala, M.; Hurst, J.; Trabjerg, I. *Mol. Phys.* **1981**, *43*, 1219.
(15) Koyanagi, M.; Terada, T. *J. Lumin.* **1991**, *48*, 391.
(16) Koyanagi, M.; Terada, T.; Nakashima, K. *J. Chem. Phys.* **1988**, *89*, 7349.
(17) Murai, H.; Minami, M.; I'Haya, Y. J. *J. Phys. Chem.* **1988**, *92*, 2120.
(18) Ohara, K.; Miura, Y.; Terazima, M.; Hirota, N. *J. Phys. Chem.* **1997**, *A101*, 605.
(19) Scaiano, J. C.; Weldon, D.; Pliva, C. N.; Martinez, L. J. *J. Phys. Chem.* **1998**, *A102*, 6898.
(20) Coenjarts, C.; Scaiano, J. C. *J. Am. Chem. Soc.* **1998**, *122*, 3635.
(21) Pownall, H. J.; Huber, J. R. *J. Am. Chem. Soc.* **1971**, *93*, 6429.
(22) Suga, K.; Kinoshita, M. *Bull. Chem. Soc. Jpn.* **1981**, *54*, 1651.
(23) Connors, R. E.; Sweeney, R. J.; Cerio, F. *J. Phys. Chem.* **1987**, *91*, 819.
(24) Gastilovich, E. A.; Klimenko, V. G.; Shigolin, D. N. *Opt. Spectrosc.* **1983**, *54*, 597.
(25) Klimenko, V. G.; Gastilovich, E. A.; Godik, V. A.; Shigolin, D. N. *Russ. J. Phys. Chem.* **1985**, *59*, 379.

(26) Gastilovich, E. A.; Val'kova, G. A.; Shigorin, D. N. *Russ. J. Phys. Chem.* **1988**, *62*, 364.
(27) Gastilovich, E. A.; Val'kova, G. A. *Russ. J. Phys. Chem.* **1988**, *62*, 1219.
(28) Griesser, H. J.; Bramley, R. *Chem. Phys.* **1982**, *67*, 361.
(29) Griesser, H. J.; Bramley, R. *Chem. Phys.* **1982**, *67*, 373.
(30) Baba, M.; Kamei, T.; Kiritani, M.; Yamauchi, S.; Hirota, N. *Chem. Phys. Lett.* **1991**, *185*, 354.
(31) Frisch, M. J.; Trucks, G. W.; Schlegel, H. B.; Scuseria, G. E.; Robb, M. A.; Cheeseman, J. R.; Zakrzewski, V. G.; Montgomery, J. A., Jr.; Stratmann, R. E.; Burant, J. C.; Dapprich, S.; Millam, J. M.; Daniels, A. D.; Kudin, K. N.; Strain, M. C.; Farkas, O.; Tomasi, J.; Barone, V.; Cossi, M.; Cammi, R.; Mennucci, B.; Pomelli, C.; Adamo, C.; Clifford, S.; Ochterski, J.; Petersson, G. A.; Ayala, P. Y.; Cui, Q.; Morokuma, K.; Malick, D. K.; Rabuck, A. D.; Raghavachari, K.; Foresman, J. B.; Cioslowski, J.; Ortiz, J. V.; Baboul, A. G.; Stefanov, B. B.; Liu, G.; Liashenko, A.; Piskorz, P.; Komaromi, I.; Gomperts, R.; Martin, R. L.; Fox, D. J.; Keith, T.; Al-Laham, M. A.; Peng, C. Y.; Nanayakkara, A.; Gonzales, C.; Challacombe, M.; Gill, P. M. W.; Johnson, B.; Chen, W.; Wong, M. W.; Andres, J. L.; Gonzalez, C.; Head-Gordon, M.; Replogle, E. S.; Pople, J. A. *Gaussian 98*, Revision A.7; Gaussian, Inc.: Pittsburgh, PA, 1998.
(32) Scott, A. P.; Radom, L. *J. Phys. Chem.* **1996**, *100*, 16502.
(33) Connors, R. E.; Fratini, C. M. *J. Mol. Struct.* **2000**, *553*, 235.
(34) Becke, A. D. *J. Chem. Phys.* **1993**, *98*, 5648.
(35) Lee, C.; Yang, W.; Parr, R. G. *Phys. Rev. B* **1988**, *37*, 785.
(36) Chappell, P. J.; Ross, I. G. *Chem. Phys. Lett.* **1976**, *43*, 440.
(37) Innes, K. K. *J. Mol. Spectrosc.* **1983**, *99*, 297.
(38) Bixon, M.; Jortner, J. *J. Chem. Phys.* **1968**, *48*, 715.